BASIC SCIENCE

Nanomedicine: Nanotechnology, Biology, and Medicine
27 (2020) 102209

Original Article

nanomedjournal.com

Dendrigraft poly-L-lysines delivery of DNA vaccine effectively enhances the immunogenic responses against H9N2 avian influenza virus infection in chickens

Kai Zhao, PhD[a,b,*], Guangyu Rong, PhD[a,b,c], Qiaoyang Teng, PhD[c], Xuesong Li, PhD[c], Hailing Lan, MD[a,b,c], Lu Yu, MD[a,b], Shuang Yu, MD[a,b], Zheng Jin, PhD[d], Guangping Chen, PhD[e,**], Zejun Li, PhD[c,**]

[a]*Engineering Research Center of Agricultural Microbiology Technology, Ministry of Education, Heilongjiang University, Harbin, China*
[b]*Key Laboratory of Microbiology, College of Heilongjiang Province, School of Life Science, Heilongjiang University, Harbin, China*
[c]*Department of Avian Infectious Disease, and Innovation Team for Pathogenic Ecology Research on Animal Influenza, Shanghai Veterinary Research Institute, Chinese Academy of Agricultural Science, Shanghai, China*
[d]*Key Laboratory of Chemical Engineering Process and Technology for High-efficiency Conversion, College of Chemistry and Material Sciences, Heilongjiang University, Harbin, China*
[e]*Department of Physiological Sciences, College of Veterinary Medicine, Oklahoma State University, Stillwater, OK, USA*

Revised 3 February 2020

Abstract

Biodegradable nanomaterials can protect antigens from degradation, promote cellular absorption, and enhance immune responses. We constructed a eukaryotic plasmid [pCAGGS-opti441-hemagglutinin (HA)] by inserting the optimized HA gene fragment of H9N2 AIV into the pCAGGS vector. The pCAGGS-opti441-HA/DGL was developed through packaging the pCAGGS-opti441-HA with dendrigraft poly-l-lysines (DGLs). DGL not only protected the pCAGGS-opti441-HA from degradation, but also exhibited high transfection efficiency. Strong cellular immune responses were induced in chickens immunized with the pCAGGS-opti441-HA/DGL. The levels of IFN-γ and IL-2, and lymphocyte transformation rate of the vaccinated chickens increased at the third week post the immunization. For the vaccinated chickens, T lymphocytes were activated and proliferated, the numbers of CD3+CD4+ and CD4+/CD8+ increased, and the chickens were protected completely against H9N2 AIV challenge. This study provides a method for the development of novel AIV vaccines, and a theoretical basis for the development of safe and efficient gene delivery carriers.

Key words: H9N2 avian influenza; Dendrigraft poly-L-lysine; Nanoparticles; Delivery of DNA vaccine; Immune responses

H9N2 subtype avian influenza virus (AIV), known as lowly pathogenic AIV (LPAIV), causes great losses in the poultry industry by causing avian eggs laying drop, respiratory diseases and successive breakouts of diseases. Moreover, H9N2 AIV provided internal genes to other subtype influenza viruses, *e.g.* H7N9, which have infected humans with high mortality rate.[1,2] Sporadic cases of H9N2 infection in humans have been reported as well. At present, vaccination is still one of the most effective measures to prevent AI, but there are some difficulties in the use of vaccines to prevent the disease because of frequently antigenic drift and shift of AIV.[3] And commercial killed H9N2 vaccine induced strong humoral antibody level, but limited cellular immune response, which caused partial protection in field. Therefore, it is significant to develop new vaccines to protect the H9N2 AIV infection.

DNA vaccines have been studied to treat many diseases caused by pathogens.[4–6] Compared to other types of vaccines, DNA vaccines exhibit several main features and advantages.

*Correspondence to: K. Zhao, Engineering Research Center of Agricultural Microbiology Technology, Ministry of Education, Heilongjiang University, Harbin 150500, China.
**Corresponding authors.
E-mail addresses: zybin395@126.com (K. Zhao), guangping.chen@okstate.edu (G. Chen), lizejun@shvri.ac.cn (Z. Li).

https://doi.org/10.1016/j.nano.2020.102209
1549-9634/

DNA vaccines are relatively safe without serious side effects,[7,8] and can be rapidly developed in a few weeks when being threatened by a pandemic pathogen and are stable at room temperature and easy to be stored and transported. Additionally, genes can also be edited by mutation or other means to enhance their immunogenicity or safety. However, DNA vaccine has drawbacks; the plasmid DNA enters the body cells less efficiently, has lower immunogenicity and is easily degraded *in vivo*.

Nanoparticles (NPs) with different compositions, sizes, shapes and surface properties have been increasingly applied in the medical field.[9,10] NPs can enter cells by endocytosis because of their smaller size and cellular composition.[11] Currently, a number of nano-scale vaccines and drug delivery systems have been developed and applied in the prevention and treatment of various diseases.[12–14] NPs can serve either as a delivery system to enhance antigen-presenting efficiency or as a vaccine adjuvant to enhance immune response.[15,16] Dendrimers are a type of highly branched, symmetrical, and radial macromolecules similar to a dendrite. Dendrimers have many features, including a large number of branch points, three-dimensional and spherical with monodisperse, and fixed nanometer size range. The characteristic three-dimensional structures of dendrimers enable them the ability to pass through cell membranes; therefore, they are better nano delivery materials than the classical polymers.[17] An expeditious multigram-scale synthesis of lysine dendrigraft polymers by aqueous *N*-carboxyanhydride polycondensation had been described.[18] Due to these unique properties, cationic dendrimers have been widely used for drug and gene delivery.[19–21]

Synthetic polymers including chitosan, polyetherimide (PEI), poly(lactic-co-glycolic acid) (PLGA), polyamidoamine (PAMAM) and poly-l-lactic acid (PLA) have been widely used in gene- and drug-delivery systems. Dendrigraft poly-l-lysines (DGLs), which are nonviral delivery vectors for drug and are entirely made of lysine, are a type of polycation dendrimer formed by poly condensation of lysine. DGL, including its central core, is composed entirely of lysine; therefore, DGL is completely biodegradable. The degradation monomer of DGL is lysine; thus, DGL is less toxic than other polymers. In addition, DGL is water-soluble, thermally stable, and non-immunogenic. Currently, DGL has been employed as drug and gene delivery vehicle due to its biodegradability and rich external amino groups that can encapsulate drugs by the emulsion crosslinking method or plasmid DNA through electric interactions.[22] The high density of terminal functional groups in G3 generation DGL can provide a large number of reaction bases for the combination of DGL with drug molecules and can control the drug through the change in pH and temperature of the lesion. The molecular size and shape of DGL are controllable; thus, DGL can be modified with targeting ligands, rendering vectors with targeting properties and long circulation.[23–25] Besides, DGL can form stable complexes with plasmid DNA and have markedly higher gene transfection abilities than the other polymers.[26,27] DGL has been widely applied in the field of antiviral, gene and drug delivery *etc.*[24–26,28–31] It had been proved that DGL had dual gene targeting delivery potential and could efficiently transport gene fragments across the blood–brain barrier.[23] However, to date, there is no report regarding whether DGL can deliver a DNA vaccine in the field of veterinary vaccines.

This study investigated the possibility of DGL as the delivery of a DNA vaccine against H9N2 AIV. It aimed (1) to evaluate the effectiveness of DGL nano delivery system for a DNA vaccine, (2) to characterize the physicochemical, toxicological, biological binding and release, immunological properties and stability of the plasmid DNA, and (3) to evaluate the ability of DGL for the delivery of DNA vaccine and determine the effectiveness of the nano vaccine in protecting chickens from infection of H9N2 AIV. We have developed the DGL nano delivery system for improving the efficiency of the DNA vaccine trans-membrane transport and expression. This new method enhanced both humoral and cellular immune responses.

Methods

Construction of the eukaryotic expression plasmid

The plasmid pCAGGS and pUC19-opti441-HA were obtained from the Laboratory of Innovation Team for Pathogen Ecology Research on Animal Influenza Virus of Shanghai Veterinary Research Institute, CAAS. Hemagglutinin (HA) of AIV has been frequently used as antigen in DNA vaccines because of its capability of inducing a broad protective immune response.[32] Therefore, we constructed a eukaryotic expression plasmid expressing HA protein (pCAGGS-opti441-HA) by using the optimized HA gene of H9N2 subtype AIV. Briefly, the plasmid pCAGGS and pUC19-opti441-HA were digested by *EcoR* I and *Xho* I. The digested fragments were then ligated by T4 DNA ligase and transformed into *E. coli* DH5α competent cells. The positive pCAGGS-opti441-HA expressing HA protein was purified using QIAGEN Plasmid Maxi Kit.

Cell culture and cytotoxicity analysis of DGL

Madin-Daby canine kidney cells (MDCK cells) and DF-1 cells were maintained in Dulbecco's modified Eagle medium (DMEM) supplemented with 10% heat-inactivated fetal bovine serum (FBS), 100 U/ml penicillin and 100 mg/ml streptomycin, and cultured at 37 °C under a humidified atmosphere containing 5% CO_2.

Dendrigraft poly-L-lysines (DGLs) (containing 123 primary amino groups, generation 3) were purchased from COLCOM (Montpellier Cedex, France). *In vitro* cytotoxicity of G3-DGL was evaluated by CCK-8 reagent (Dojindo, Kumamoto, Japan). The survival rate of DF-1 cells was determined by measuring optical density at 450 nm (OD450). Briefly, DF-1 cells were diluted to the final cell concentration of 2×10^5 cells/ml, transferred to 96-well plates at 100 μl per well, and cultured at 37 °C for 16 h. Cells were treated with different concentrations of DGL after being rinsed once with PBS. After 4 h incubation, DGL solutions were removed, and the cells were continuously cultured for an additional 40 h. Then, 10 μl of CCK-8 reagents was added and incubated for another 4 h. The OD450 was read with a microplate reader. Cells without any treatment were set as 100% viability. All measurements were performed in quintuplicate.

Synthesis of the pCAGGS-opti441-HA/DGL

The pCAGGS-opti441-HA/DGL was synthesized by the electrostatic interaction of NH_3^+ in DGL and PO_4^- in nucleic acids (pCAGGS-opti441-HA or EGFP plasmid) in distilled water at various N/P ratios. The mixture was incubated at room temperature for 30 min. The linkage of DGL with the plasmid was detected by 0.8% agarose gel at 90 V for 40 min. The transfection efficiency of DGL was detected *via in vitro* transfection assay. The mixture was transfected into DF-1 cells grown in 96-well plates at 37 °C in a CO_2 (5%) incubator. The cells were analyzed when the cell growth reached around 80% confluence. After the cells were incubated with the mixture for 24 h, epifluorescence images were acquired using a fluorescent microscopy (Zeiss, Oberkochen, Germany). The size and zeta potentials of the resulting pCAGGS-opti441-HA/DGL were measured by Zeta Sizer 2000 from Malvern Instruments (Malvern, UK).

DNase I protection assay

To test the stability of pCAGGS-opti441-HA/DGL against DNase hydrolysis, 6 μl of pCAGGS-opti441-HA/DGL (equivalent to 3.0 μg of the naked plasmid DNA) was incubated with 3 U of DNase I (TransGen Biotech, China) at 37 °C in 10 μl of reaction buffer for 30 min. The reaction was terminated by adding 0.5 μl of EDTA (200 μM) at 65 °C for 10 min. Then the reaction samples were examined by 1% agarose gel with TAE buffer containing 1% ethidium bromide at 100 V for 40 min.

In vitro expression

To verify *in vitro* expression of pCAGGS-opti441-HA mixed with DGL, MDCK cells were seeded at a density of 1×10^4 cells/well at 37 °C and 5% CO_2. The cells were incubated with the pCAGGS-opti441-HA/DGL containing media (without serum) at 37 °C for 24 h when the cells growth reached 80% confluence. The expression of HA protein in the transfected cells was monitored with an indirect immuno-fluorescent test. The H9N2 AIV positive serum (Shanghai Veterinary Research Institute, China) and fluorescein isothiocyanate-labeled goat-anti-chicken IgG (Sigma, St. Luis, MO, USA) were used at a dilution of 1:500 and 1:500, respectively. The cell nuclei were stained with the 4′,6-diamidino-2-phenylindole (DAPI, Roche, Basel, Switzerland) for 5 min at room temperature. Epifluorescence images were acquired using a laser scanning confocal microscope (Nikon, Japan).

In vitro release and stability

To test the release of pCAGGS-opti441-HA from the pCAGGS-opti441-HA/DGL, 200 μl of the pCAGGS-opti441-HA/DGL containing 200 μg of the pCAGGS-opti441-HA was mixed with 10.0 ml PBS solution containing 0.25 mmol/l glucose, and then vibrated on a shaker at 37 °C. The samples were collected at different time point and the DNA concentration was measured on a spectrophotometer. Additionally, to evaluate the stability of pCAGGS-opti441-HA/DGL during the storage, these nanoparticles were placed at room temperature for 1 h, 2 h, 6 h, 12 h, 24 h, 72 h and 120 h, respectively. Their morphological changes and particle size were observed and recorded. All experiments were repeated at least twice.

Table 1
HI antibody in SPF chickens inoculated with vaccines.

Groups	Immunization grouping	Weeks post the immunization Weeks					
		1	2	3	4	5	6
1	pCAGGS-opti441-HA/DGL i.m.	0/8	7/8	7/8	7/8	7/8	7/8
2	pCAGGS-opti441-HA i.m.	0/8	3/8	3/8	5/8	5/8	7/8
3	pCAGGS-opti441-HA/DGL i.m.e.	0/8	5/8	5/8	5/8	5/8	7/8
4	pCAGGS-opti441-HA i.m.e.	0/8	5/8	6/8	6/8	6/8	8/8
5	pCAGGS-opti441-HA/DGL i.n.	0/8	0/8	0/8	0/8	0/8	0/8
6	pCAGGS-opti441-HA i.n.	0/8	0/8	0/8	0/8	0/8	0/8
7	DGL i.n.	0/5	0/5	0/5	0/5	0/5	0/5
8	PBS i.n.	0/5	0/5	0/5	0/5	0/5	0/5
9	DGL i.m.	0/5	0/5	0/5	0/5	0/5	0/5
10	PBS i.m.	0/5	0/5	0/5	0/5	0/5	0/5
11	DGL i.m.e.	0/5	0/5	0/5	0/5	0/5	0/5
12	PBS i.m.e.	0/5	0/5	0/5	0/5	0/5	0/5

In vivo biological safety assay

For the *in vivo* biological safety assay, nine 4-week-old specific pathogen free (SPF) chickens obtained from Shanghai Veterinary Research Institute were randomly grouped into three groups with 3 chickens in each group. Chickens in Group 1 were immunized intramuscularly (i.m.) with 1.0 ml of pCAGGS-opti441-HA/DGL containing a total of 2 mg of the pCAGGS-opti441-HA and the N/P ratio was 3; chickens in Group 2 were immunized intramuscularly electronic transfer (i.m.e.) with 1 ml of the pCAGGS-opti441-HA/DGL and the N/P ratio was same as Group 1; chickens in Group 3 were immunized i.m. with phosphate buffered saline (PBS, pH 7.4). Any abnormal changes in chickens were continuously observed and recorded for 14 days.

Immunization and challenge

78 three-week-old healthy SPF chickens were randomly divided into three groups with 26 chickens in each group, and each group was divided into four subgroups. Chickens in Group 1 were immunized i.m. with the pCAGGS-opti441-HA/DGL (containing 200 μg of the pCAGGS-opti441-HA, 8 chickens), 200 μg of the pCAGGS-opti441-HA (8 chickens), DGL (5 chickens) and PBS (5 chickens), respectively. Chickens in Group 2 were immunized i.m.e. with the pCAGGS-opti441-HA/DGL (8 chickens), 200 μg of the pCAGGS-opti441-HA (8 chickens), DGL (5 chickens) and PBS (5 chickens), respectively. Chickens in Group 3 were immunized intranasally (i.n.) with the pCAGGS-opti441-HA/DGL (8 chickens), 200 μg of the pCAGGS-opti441-HA (8 chickens), DGL (5 chickens) and PBS (5 chickens), respectively. The groups and immune method of chickens are shown in Table 1. Four weeks after the first immunization, chickens were given another shot using the same formula. Two weeks after the last immunization, chickens were challenged with 100 μl of viral suspension containing 10^6 EID_{50}/0.1 ml of H9N2 (Ck/Shanghai/441/2009) viruses *via*

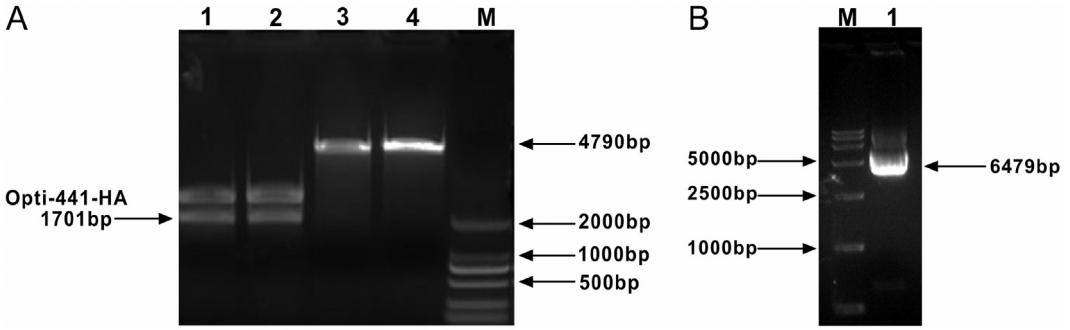

Figure 1. **(A)** The enzymatic digestion analysis of pCAGGS and Opti-441-HA. M: DNA marker DL 2000; lanes 1 and 2: opti-441-HA digested by enzyme; lanes 3 and 4: pCAGGS digested by enzyme. **(B)** The identification of pCAGGS-opti-441HA by agarose gel electrophesis. M: DL 15000 Marker; 1: pCAGGS-opti-441-HA.

intravenous infusion. Oropharyngeal (OP) and cloacal (CL) swabs were collected from all the chickens at day 3, 5 and 7 post-infection. The viral titers of swabs were detected as previously described.[1] Survival rates of chickens were monitored for 7 days. All animal experiments were conducted in accordance with Animal Ethics Guidelines and Protocols approved by the Animal Ethics Committee of the Shanghai Veterinary Research Institute of the Chinese Academy of Agricultural Sciences, China (shvri-ro-2,015,040,384).

Assays of hemagglutination inhibition antibody and cytokines

To assess immune response of immunized chicken, chickens of each group were bled weekly and serum samples were separated from the blood. The titers of AIV (H9N2) HI antibody were detected by hemagglutination inhibition (HI) assay as previously described.[33] The levels of IFN-γ and IL-2 in serum were determined using an ELISA Kit (Enzyme-linked Biotechnology Co. Ltd., Shanghai, China). All the operations were performed according to the procedures described for the cytokine ELISA Kits.

Assay of lymphocyte proliferation

The peripheral blood mononuclear cells (PBMCs) of chickens were purified from heparinized blood by using Ficoll density gradient centrifugation method. Briefly, the blood was diluted 1:1 with PBS and layered onto lymphocyte separation liquid (TBD Science, Tianjin, China) and then centrifuged at 500 ×g for 30 min. The PBMC-containing interface was subsequently transferred to new tubes and washed twice with PBS containing 0.5% FBS by centrifugation at 250 ×g for 5 min. The PBMCs were re-suspended in RPMI1640 supplemented with 10% FBS and the cell concentration was adjusted to 2.5×10^6 cells/ml. 80 μl of cell suspension (2×10^5 cells/well) was cultured in 96-well plate and stimulated with 20 μl of ConA (50 μg/ml). Medium alone was taken as the negative control. The plates were cultured at 37 °C for 44 h. The stimulation indexes (SIs) were assayed with CCK-8 reagent.

Flow cytometric analysis

PBMCs of chickens were collected and the diversity of CD4+/CD8+ was detected. Briefly, 1×10^6 PBMCs were incubated with mouse anti chicken CD3-SPRD, anti-chicken CD4-FITC, and anti-chicken CD8α-PE (Southern Biotech, Birmingham, AL, USA) at room temperature for 20 min. Isotype controls produced by incubating PBMCs with mouse IgG1 (Southern Biotech, Birmingham, AL, USA) conjugated to SPRD, FITC and PE. The cells were washed twice with FACS buffer (Bioscience, San Diego, CA, USA), then suspended with FACS buffer and analyzed by the CytomicsTM FC 500 (Beckman Coulter, Indianapolis, Indiana, USA).

Statistical analysis

All the results were expressed as mean values ± standard deviation (SD). All experiments were repeated for at least three times with at least triplicated samples in each experiment. Kruskal-Wallis one-way analysis of variance (ANOVA) was employed to evaluate the statistical differences among different groups with SPSS 19.0 software. The difference between groups with P value of $<.05$ was considered to be statistically significant.

Results

Construction of pCAGGS-opti-441-HA

After being double digested with *EcoR* I and *Xho* I, the Opti-441-HA fragment (1701 bp) was obtained and the band size was in line with the expected results (Figure 1, *A*). After the digestion, the Opti-441-HA fragment was ligated with the pCAGGS fragment. Figure 1, *B* demonstrated the construction of the pCAGGS-opti441-HA.

Preparation and characterization of pCAGGS-opti441-HA/DGL

It can be seen from Figure 2, *A* that when N/P is 1.5, no pCAGGS-opti441-HA is seen escaping, indicating that the minimum N/P ratio of DGL to pCAGGS-opti441-HA is 1.5. In Figure 2, *B*, when N/P is 3.0, the fluorescence density is higher than the low N/P ratio. As the N/P ratio increases, the increasing

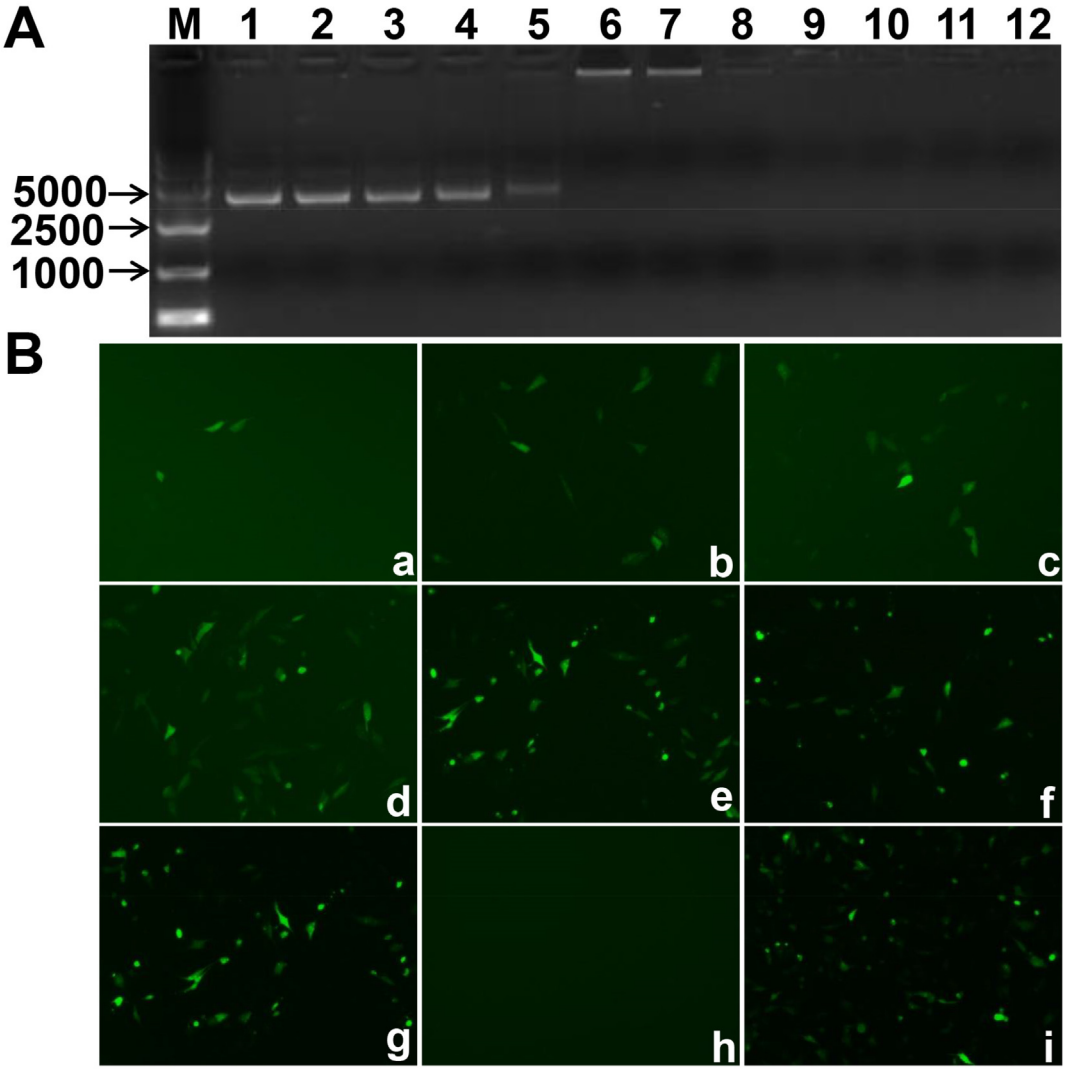

Figure 2. **(A)** Identification of DGL and pCAGGS-opti-441-HA in different N/P ratio by agarose gel electrophesis. M: DL 15000 Marker; lane 1: pCAGGS-opti-441-HA. lanes 2-12: N/P ratios of DGL and pCAGGS-opti-441-HA were 0.1, 0.2, 0.5, 1.0, 1.5, 2.0, 2.5, 3.0, 4.0, 5.0 and 8.0, respectively. **(B)** Identification of DGL and EGFP in difference N/P ratios by *in vitro* transfection test. a-g: N/P ratios of DGL to EGFP were 1.0, 1.5, 2.0, 3.0, 4.0, 5.0 and 8.0, respectively; h: transfection of naked EGFP; i: transfection of commercial transfection reagent and EGFP.

fluorescence trend is nearly saturated, indicating that the optimal N/P ratio of DGL to pCAGGS-opti-441-HA is 3.0.

The pCAGGS-opti441-HA/DGL prepared by the optimal N/P ratio (N/*P* = 3.0) displayed uniform morphology and good dispensability (Figure 3, *A*), the average particle size was 68.9 ± 2.1 nm (Figure 3, *B*), and the average zeta potential was 55.1 ± 1.3 mV (Figure 3, *C*). In addition, dynamic light scattering (DLS) by number and volume distribution and the characterization for all N/P ration optimization regarding size and zeta potential can be seen in Supplementary Information (Figure S1).

Biological safety of DGL and pCAGGS-opti441-HA/DGL

As shown in Figure 4, *A*, when DGL concentrations 0.1, 1.0, and 10 μg/ml were used to treat the cells for 4 h, there were no significant difference in cell survival rate ($P > 0.05$) compared to control group, indicating that DGL showed minimal toxicity on the cells under 10 μg/ml. When DGL concentration was increased to 100 μg/ml, the cell viability was 82.2 ± 0.1% ($P < 0.05$).

To evaluate the safety of pCAGGS-opti441-HA/DGL, SPF chickens were divided into four groups with 3 in each group. The pCAGGS-opti441-HA/DGL dose used here was 10 times higher than that used for chicken immunization treatment. After two weeks of observation, there were no abnormal symptoms for all the chickens treated in the four groups; no sickness and no death happened. Necropsy examination also showed no differences between the four groups. These results suggest that the pCAGGS-opti441-HA/DGL is not noticeable toxic to SPF chickens.

Protection of DGL against the DNaseI digestion of the pCAGGS-opti441-HA

DNaseI digestion of the pCAGGS-opti441-HA/DGL was shown in Figure 4, *B*. The naked pCAGGS-opti441-HA could be

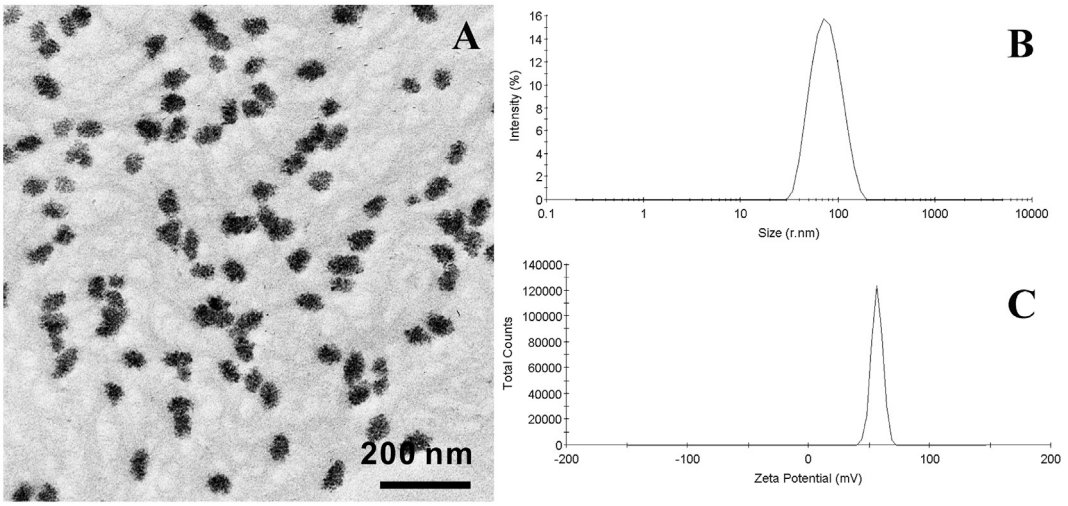

Figure 3. TEM morphology **(A)**, particle size distribution **(B)** and zeta potential **(C)** of the pCAGGS-opti441-HA/DGL.

digested by DNaseI in 30 min. However, the pCAGGS-opti441-HA was resistant to the digestion of DNaseI after being mixed with DGL. The pCAGGS-opti441-HA could be released from the DNaseI treated pCAGGS-opti441-HA/DGL by heparin sodium. These results suggest that DGL can protect the plasmid from being digested by DNaseI.

In vitro HA protein expression of the pCAGGS-opti441-HA/DGL

As shown in Figure 4, *C* and Figure 4, *D*, no fluorescence was detected under microscope in the control MDCK cells (Group D) and the pCAGGS-opti441-HA treated MDCK cells (Group C), indicating that no HA protein was expressed under these conditions. However, for the pCAGGS-opti441-HA/DGL treated MDCK cells (Group A), strong fluorescence was detected, indicating that the pCAGGS-opti441-HA was transfected into the cells by DGL, and HA protein was expressed. When MDCK cells were treated with DNase I digested pCAGGS-opti441-HA/DGL (Group B), strong fluorescence was also detected, indicating that DGL not only transfected the plasmid into the cells, but also protected the plasmid from being hydrolyzed by nuclease.

In vitro release and stability of the pCAGGS-opti441-HA from pCAGGS-opti441-HA/DGL

As shown in Figure 4, *E*, the plasmid *in vitro* release was slow within the first 24 h. A burst release was followed between 24 and 72 h (reached 69.3 ± 2.5% at 72 h). The plasmid DNA sustained slow release between 72 and 216 h (reached 81.0 ± 4.4% at 216 h). Additionally, the stability of the nanoparticles at the room temperature for 1 h, 2 h, 6 h, 12 h, 24 h, 72 h and 120 h was evaluated, respectively. The results showed that no significant changes in the morphology and particle size of nanoparticles were observed, indicating that the nanoparticles are stable and can be stored for a long period of time even at the room temperature (Figure S2).

HI antibody in SPF chickens inoculated with vaccines

No HI antibody was produced in chickens of all 12 groups at the first week post the immunization (Table 1). 7 out of 8 chickens were HI positive against H9N2 in pCAGGS-opti441-HA/DGL i.m. in the second week post the immunization; the positive rate was 87.5% (7/8). In the sixth week post the immunization, the positive rate of pCAGGS-opti441-HA i.m.e group was 100% (8/8), whereas no HI antibody was detected in chickens in the pCAGGS-opti441-HA/DGL i.n. and pCAGGS-opti441-HA i.n. groups.

Figure 5, *A* showed that no HI antibody was produced in chickens in all eight groups at the first week post the immunization; HI antibody levels in the pCAGGS-opti441-HA/DGL i.m. were higher than those of chickens in other groups. The HI antibody levels in chickens in the pCAGGS-opti441-HA i.m. and pCAGGS-opti441 groups were significantly different compared to those chickens in the pCAGGS-opti441-HA/DGL group ($P < 0.05$). In the second week after the booster immunization, there was an increase in HI antibody levels in the pCAGGS-opti441-HA/DGL i.m., pCAGGS-opti441-HA i.m., pCAGGS-opti441-HA/DGL i.m.e. and pCAGGS-opti441-HA groups.

Peripheral blood lymphocyte proliferation of immunized chickens

As shown in Figure 5, *B*, the increase in SIs of peripheral blood lymphocytes was not significant in the second week post the immunization, but the levels in the pCAGGS-opti441-HA/DGL i.m.e. were higher than those of the other groups, indicting the nano vaccine has not yet effectively stimulated the body to produce a strong cellular immune response. The SIs of pCAGGS-opti441-HA/DGL i.m. and pCAGGS-opti441-HA i.

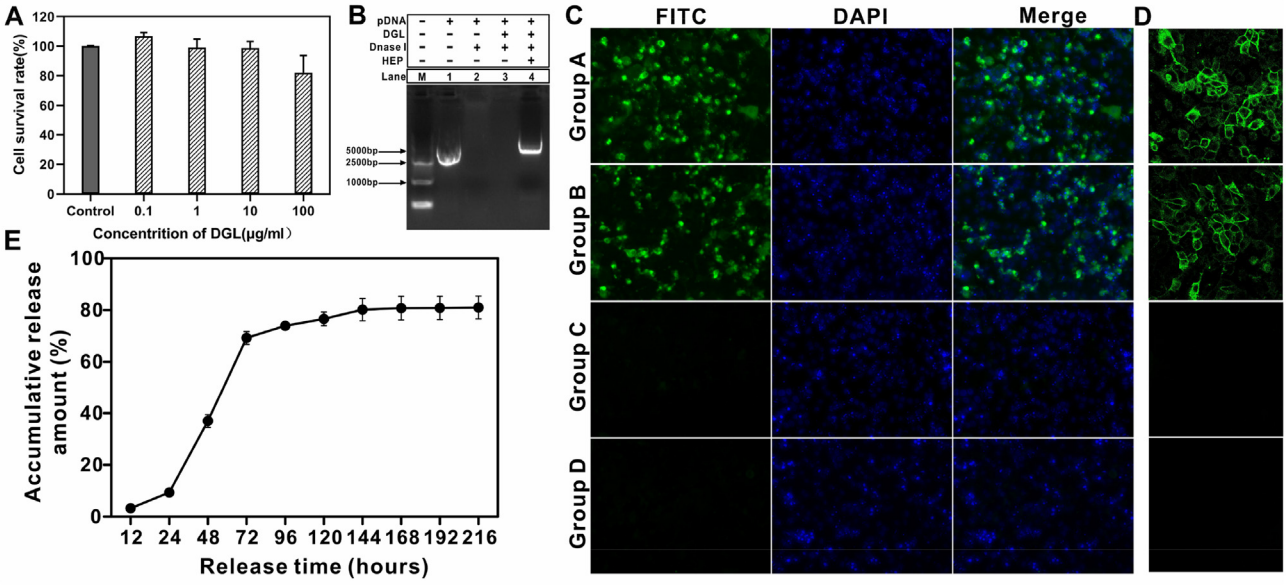

Figure 4. **(A)** Toxic effects of DGL at different concentrations on DF-1 cells; **(B)** DNase I protection assay. M: DL 15000 marker; lane 1: plasmid DNA; lane 2: plasmid DNA digested with DNase I for 30 min; lane 3: pCAGGS-opti441-HA/DGL digested with DNaseI for 30 min; lane 4: heparin sodium was added after pCAGGS-opti441-HA/DGL was digested with DNaseI for 30 min. **(C & D)** Indirect immunofluorescence LSCM image of pCAGGS-opti441-HA/DGL (×20). Group A: transfection of pCAGGS-opti441-HA/DGL; Group B: transfection of pCAGGS-opti441-HA/DGL that deal with DNaseI; Group C: transfection of naked pCAGGS-opti-441-HA; Group D: MDCK cells control. **(E)** Release curve of pCAGGS-opti441-HA/DGL *in vitro*.

m. were significantly increased at the 4th weeks post the immunization with ConA ($P < 0.01$). The level of SIs was not significantly changed at the pCAGGS-opti441-HA/DGL i.m. for 6 weeks post the immunization. The difference was significant ($P < 0.01$) as compared with those of DGL and PBS groups. The results suggest that intramuscular immunization of chickens with pCAGGS-opti441-HA/DGL effectively stimulates lymphocyte transformation and promotes the cellular immune responses.

Duration of immunity

Based on the results of animal immunization, the pCAGGS-opti441-HA/DGL i.m. and pCAGGS-opti441-HA/DGL i.m.e. and H9 subtype inactivated vaccine (SD696 strain) i.m. were selected to determine the duration of vaccine immunization. As shown in Figure 5, *C*, HI antibody levels in chicken of all but PBS groups were significantly increased in the second week post the immunization. HI antibody levels of the pCAGGS-opti441-HA/DGL i.m and pCAGGS-opti441-HA i.m.e. were not significantly different ($P > 0.05$), while HI antibody titers of the pCAGGS-opti441-HA/DGL i.m. and pCAGGS-opti441-HA i.m.e. peaked at week 6 and continued to gradually decline until week 12. HI antibody levels of chickens in H9 subtype inactivated vaccine i.m. were significantly higher than those of the other groups ($P < 0.01$).

Recover of H9N2 avian influenza virus in chickens after challenge

After intravenous injection of chickens with 10^6 EID_{50}/0.1 ml H9N2 AIV (Table 2), the virus was not detected in the laryngeal and cloacal swabs of the chickens immunized by the pCAGGS-opti441-HA/DGL i.m., or pCAGGS-opti441-HA i.m., while the higher titer of virus was isolated from the chickens treated with DGL, PBS, indicating that pCAGGS-opti441-HA/DGL is capable of protecting SPF chickens from H9N2 AIV infection.

The virus could be isolated from the oropharyngeal swabs of all the immunized chickens on days 3 and 5 after being challenged through the nose (Table 3), but the viral titers in chickens vaccinated with pCAGGS-opti441-HA/DGL i.m., pCAGGS-opti441-HA i.m., pCAGGS-opti441-HA/DGL i.m.e. and pCAGGS-opti441-HA i.m.e. were lower than those of chickens in DGL i.m., PBS i.m., PCAGGS-opti441-HA/DGL i.n. and pCAGGS-opti441-HA i.n. groups. No virus was isolated in oropharyngeal swabs of all the chickens vaccinated with pCAGGS-opti441-HA/DGL i.m., pCAGGS-opti441-HA i.m., pCAGGS-opti441-HA/DGL i.m.e. and pCAGGS-opti441-HA i.m.e. groups on day 7.

No virus was isolated in the cloacal swabs of all the chickens vaccinated with pCAGGS-opti441-HA/DGL i.m., pCAGGS-opti441-HA i.m., pCAGGS-opti441-HA/DGL i.m.e. and pCAGGS-opti441-HA i.m.e. on days 3, 5 and 7 after being challenged through the nose. These results suggest that the pCAGGS-opti441-HA/DGL i. m. induced the higher level of HI antibody against H9N2 AIV and a higher level of immune protective effect on SPF chickens was achieved after intravenous injection of H9N2 AIV.

Induction of cytokines

As shown in Figure 6, *A*, IL-2 levels were not significant in the first two weeks post 1st immunization; IL-2 levels in the

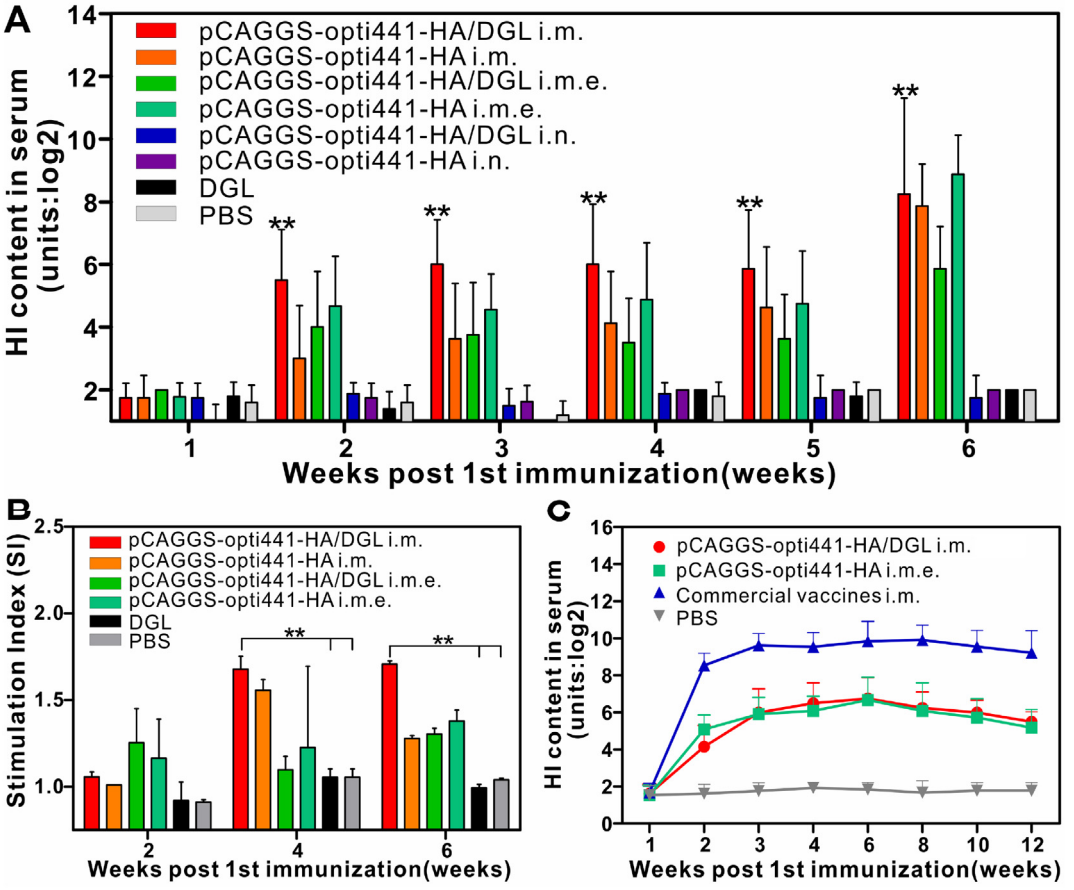

Figure 5. Serum IgG antibody titers. **(A)**, changes of peripheral blood lymphocyte proliferation **(B)** and duration of immunity **(C)**, post 1st immunization. Values represent mean ± S.D. $^{**}P < 0.01$ was significantly different.

pCAGGS-opti441-HA/DGL i.m. reached the highest values at the third week. IL-2 levels in the pCAGGS-opti441-HA/DGL i.m. were significantly higher than those compared to PBS group ($P < 0.01$) at 3, 4, 5 and 6 weeks post the 1st immunization. The pCAGGS-opti441-HA/DGL i.m. and pCAGGS-opti441-HA/DGL i.m.e. showed no significant difference in IL-2 levels (Figure 6, *A*).

IFN-γ levels were not changed significantly in the first two weeks after immunization (Figure 6, *B*) for all groups. IFN-γ levels in the pCAGGS-opti441-HA/DGL i.m. and pCAGGS-opti441-HA/DGL i.m.e. were significantly increased at the third week after immunization compared to PBS and DGL groups ($P < 0.01$).

Changes of CD3+, CD4+, CD8+ levels in peripheral blood

The levels of induced T lymphocyte (CD3+/CD4+) in the pCAGGS-opti441-HA/DGL i.m. group and pCAGGS-opti441-HA i.m.e. were significantly higher than those in PBS ($P < 0.05$) 4 weeks post the primary immunization (Figure 7, *A*). The changes of CD4+/CD8+ levels in the first two weeks post the primary immunization (Figure 7, *B*) were not significant. CD4+/CD8+ levels in T lymphocytes of pCAGGS-opti441-HA/DGL i.m. and pCAGGS-opti441-HA i.m.e. were increased significantly 3 weeks post the primary immunization compared to that of PBS group ($P < 0.01$). There was no significant difference in CD4+/CD8+ between pCAGGS-opti441-HA/DGL i.m. and pCAGGS-opti441-HA i.m.e. ($P > 0.05$).

Discussion

To enhance the expression efficacy of HA gene, HA gene of H9N2 subtype bird flu virus isolated from chicken was optimized and cloned into the pCAGGS.[34] The pCAGGS has been known to be highly expressed in eukaryotic cells because its sequence contains the β-actin promoter and CMV enhancer of chickens.[35] Using the optimized H9 gene, we constructed the pCAGGS-opti441-HA that expressed HA protein.

The particle size of nanoparticles has been known to affect the degree of endocytosis and phagocytosis. NPs < 500 nm are usually endocytosed, whereas those >500 nm are usually intrinsic phagocytosis.[36] Endothelial cells can engulf larger particles (>5 μm).[37,38] In the present study, we selected the G3-DGL as the carrier; G3-DGL is a dendrimer polymerized from 123 lysine residues with diameter of 7 nm. Through electrostatic adsorption, DGL can be well combined with the negatively charged plasmid DNA to form the complex,

Table 2
Virus shedding and titers from chickens immunized with vaccines after challenge with virus through intravenous injection ($log_{10}EID_{50}$/ml).

Immunization grouping	Day 3		Day 5		Day 7	
	O	C	O	C	O	C
pCAGGS-opti441-HA/DGL i.m.	−	−	−	−	−	−
pCAGGS-opti441-HA i.m.	−	−	−	−	−	−
pCAGGS-opti441-HA/DGL i.m.e.	−	−	−	−	−	−
pCAGGS-opti441-HA i.m.e.	−	−	−	−	−	−
pCAGGS-opti441-HA/DGL i.n.	3.25-4.33	+	+	+	−	−
pCAGGS-opti441-HA i.n.	2.5-4.5	+	1.25-1.75	+	−	−
DGL	3.5-4.5	+	1.0-1.75	+	+	−
PBS	3.5-4.75	+	1.5-3.25	+	−	+

"O" stands for oropharyngeal swab samples; "C" stands for cloacal swab samples; "+" stands for swab sample is positive in virus isolation; "−" stands for swab sample is negative in virus isolation.

Table 3
Virus shedding and titers from chickens immunized with vaccines after being challenged through the nose (titer: $log_{10}EID_{50}$/ml).

Immunization grouping	Day 3		Day 5		Day 7	
	O	C	O	C	O	C
pCAGGS-opti441-HA/DGL i.m.	1.0-3.75	−	1.5-2.25	−	−	−
pCAGGS-opti441-HA i.m.	2.55-4.25	−	1.5-3.17	−	−	−
pCAGGS-opti441-HA/DGL i.m.e.	2.63-4.3	−	1.25-3.5	−	−	−
pCAGGS-opti441-HA i.m.e.	2.5-4.75	−	1.25-3.5	−	−	−
pCAGGS-opti441-HA/DGL i.n.	3.5-4.5	+	1.75-4.25	+	+	−
pCAGGS-opti441-HA i.n.	3.5-5.0	+	2-4.25	+	+	+
DGL	3.5-4.25	+	2.25-3.5	+	+	−
PBS	3.75-5.25	+	2.25-3.5	+	+	+

"O" stands for oropharyngeal swab sample; "C" stands for cloacal swab sample; "+" stands for swab sample is positive in virus isolation; "−" stands for swab sample is negative in virus isolation.

protecting the plasmid DNA effectively without destroying its antigenic activity. Thus, we prepared the DGL-DNA complexes with different N/P ratios and determined the optimal ratio. More importantly, within the complex, the pCAGGS-opti441-HA can be encapsulated into DGL to form a DNA vaccine. Moreover, the DGL efficiently transfected the pCAGGS-opti441-HA into DF-1 cells, and the HA protein was expressed in cells, suggesting that DGL is a functional carrier for plasmid DNA.

We examined the stability of the pCAGGS-opti441-HA/DGL and found that it was almost completely resistant to DNase I degradation under physiological pH conditions. The pCAGGS-opti441-HA/DGL treated with or without DNase I was used to transfect MDCK cells; no difference in the expression level of HA protein was seen between the two treatments, indicating that the expression of HA protein and its biological activity of plasmid DNA were not affected by adding DGL. We detected the release of pCAGGS-opti441-HA/DGL at the physiological pH and found that during 0-216 h, the plasmid DNA was released in a process from slow release to sudden burst to steady release, and the majority of the plasmid DNA was released between 24 to 72 h.

Intramuscular immunization of SPF chickens with the pCAGGS-opti441-HA/DGL produced high level of HI antibodies; it was significantly higher than those of the intramuscular injection of plasmid DNA. Furthermore, after the booster immunization with the same dose, the antibody level was further increased. The pCAGGS-opti441-HA/DGL can protect the SPF chickens from being infected by H9N2 AIV. After being challenged, the SPF chickens in the pCAGGS-opti441-HA/DGL i.m. group showed no symptoms, and no virus was detected in the cloaca swabs. The antibodies in the pCAGGS-opti441-HA/DGL i.m. persisted for up to 12 weeks after a single immunization with SPF chickens. Our results also suggest that electrically assisted intramuscular injection of the naked plasmid DNA can also effectively stimulate the body to produce humoral immune response and a longer duration of immunity, but the complex route of vaccination limits its advantages.

One of the mechanisms underlying the protection of SPF chickens from H9N2 AIV *via* intramuscular immunization with the pCAGGS-opti441-HA/DGL can be attributed to enhanced cellular immune system. The cellular immune system can be evaluated with proliferative stimulator by measuring lymphocyte proliferation. In this study, after being intramuscularly immunized with the pCAGGS-opti441-HA/DGL, the peripheral blood lymphocytes of SPF chickens exhibited significantly higher levels of proliferation after booster immunization and showed more obvious stimulatory response to ConA than other groups did, indicating that intramuscular injection of pCAGGS-opti441-HA/DGL can effectively induce a strong cellular immune response. Simultaneously, SPF chickens immunized with the pCAGGS-opti441-HA/DGL significantly enhanced the expression of pro-inflammatory cytokines. IFN-γ and IL-2 are important cytokines regulating the immune response of the body, and play a key role in the cellular immune response.[39–42] Therefore, their secreted levels can reflect the cellular immune response. In this study, the levels of IFN-γ and IL-2 in the pCAGGS-opti441-HA/DGL i.m. were significantly higher than that in the control group. The nano DNA vaccine promoted IFN-γ secretion after having entered the body, which, in turn, further promoted the antigen presenting effect and enabled the plasmid DNA to be effectively and quickly presented to T cells. The increased levels of INF-γ and IL-2 demonstrate that the nano DNA vaccine stimulates the proliferation, activates T-lymphocytes and thus, enhances the body's cellular immune function.

Additionally, immunization of SPF chickens with the pCAGGS-opti441-HA/DGL significantly enhanced the subpopulations of T lymphocytes and immune functions. The major histocompatibility complex (MHC) is a type of cell surface protein essential for recognition of foreign molecules in the acquired immune system. MHC gene family includes three types of molecules: MHC I, MHC II, and MHC III. Among them, MHC I recognizes CD8+ surface antigens and mediates the host exposure through interaction with CD8+ on the surface of cytotoxic T cells; MHC II mediates the

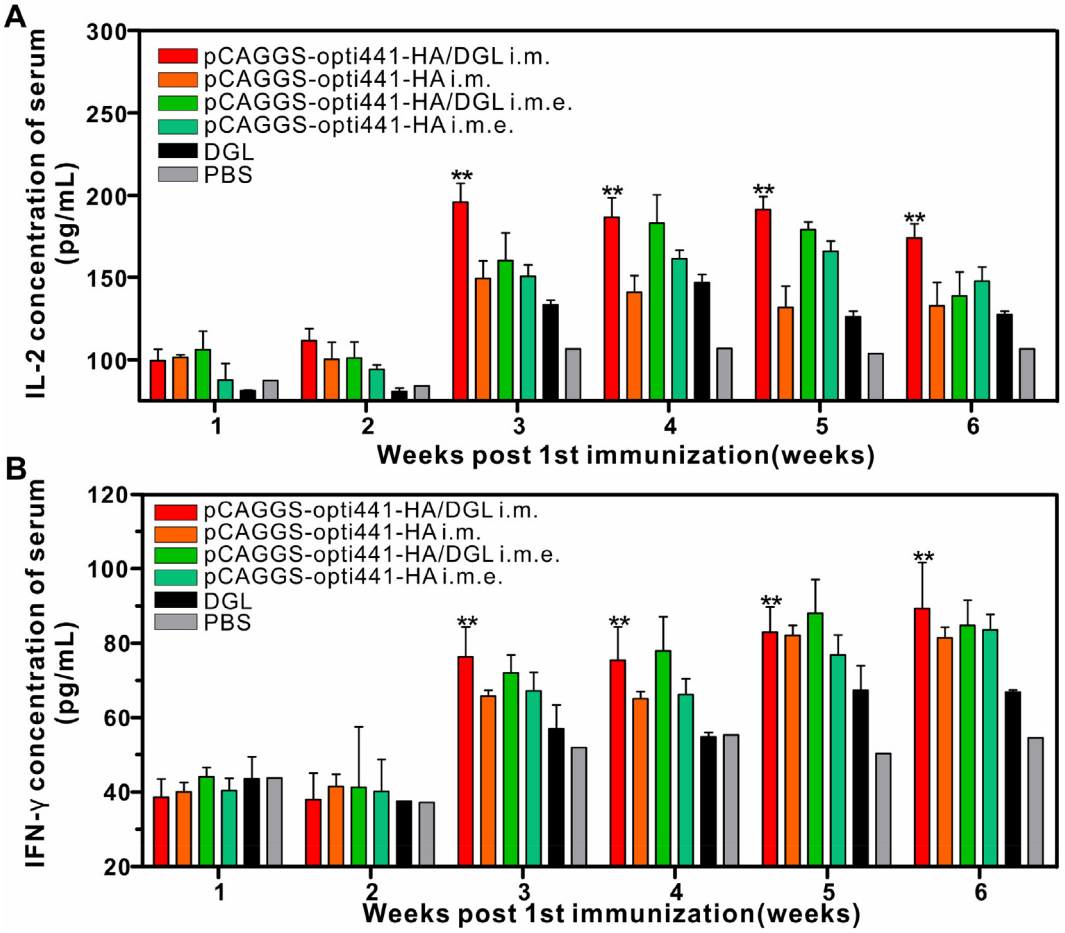

Figure 6. IL-2 **(A)** and IFN-γ **(B)** levels in serum from the SPF chickens immunized with the pCAGGS-opti441-HA/DGL i.m., pCAGGS-opti441-HA i.m., pCAGGS-opti441-HA/DGL i.m.e., pCAGGS-opti441-HA i.m.e., DGL i.m and PBS i.m. IFN-γ, IL-2 and IL-4 levels in serum were analyzed in a chicken IFN-γ and IL-2 enzyme-linked immunosorbent assay. Values represent mean ± S.D. $^{**}P < 0.01$ was significantly different.

establishment of body-specific immunity through the interaction of CD4+ molecules on the surface of helper T cells (Th). The body's immune function can be evaluated by measuring the relative contents of T lymphocyte subsets in the body.[43] CD4+ T lymphocytes are capable of enhancing the immune response; CD8+ T lymphocytes play an important role in viral clearance.[44] Therefore, changes in the levels of CD4+ and CD8+ T lymphocytes are closely related to immune function.[45,46] In our study, CD8+ and CD4+ T lymphocytes were measured, and the levels of CD3+/CD4+ and CD4+/CD8+ T lymphocytes in the pCAGGS-opti441-HA/DGL i.m. and pCAGGS-opti441-HA i.m.e. were significantly higher than those in PBS group. These results indicate that the nano DNA vaccine can effectively stimulate the body to produce both humoral and cellular immunity. Increased levels of cytokines, proliferation of T lymphocytes, and CD4+/CD8+ values demonstrated that DGL can help the plasmid DNA escape from endosomes when the pCAGGS-opti441-HA/DGL enters the body. DGL prevents the plasmid DNA degradation, increases its replication and expression in the body, promotes antigen presentation, proves the expression of the antigen protein, and stimulates the body to produce immune responses.

Acknowledgments

We gratefully acknowledge the Heilongjiang Provincial Key Laboratory of Plant Genetic Engineering and Biological Fermentation Engineering for Cold Region to carry out this work. This work was supported by the National Key Research and Development Program of China (2016YFD0500204), National Natural Science Foundation of China (31771000, 31472206), Excellent Youth Natural Science Foundation of Heilongjiang Province of China (JC2018008) and Cultivation Project of Scientific and Technological Achievements for Provincial Universities in Heilongjiang (TSTAU-C2018017).

Declaration of competing interest

The authors declare no competing financial interest.

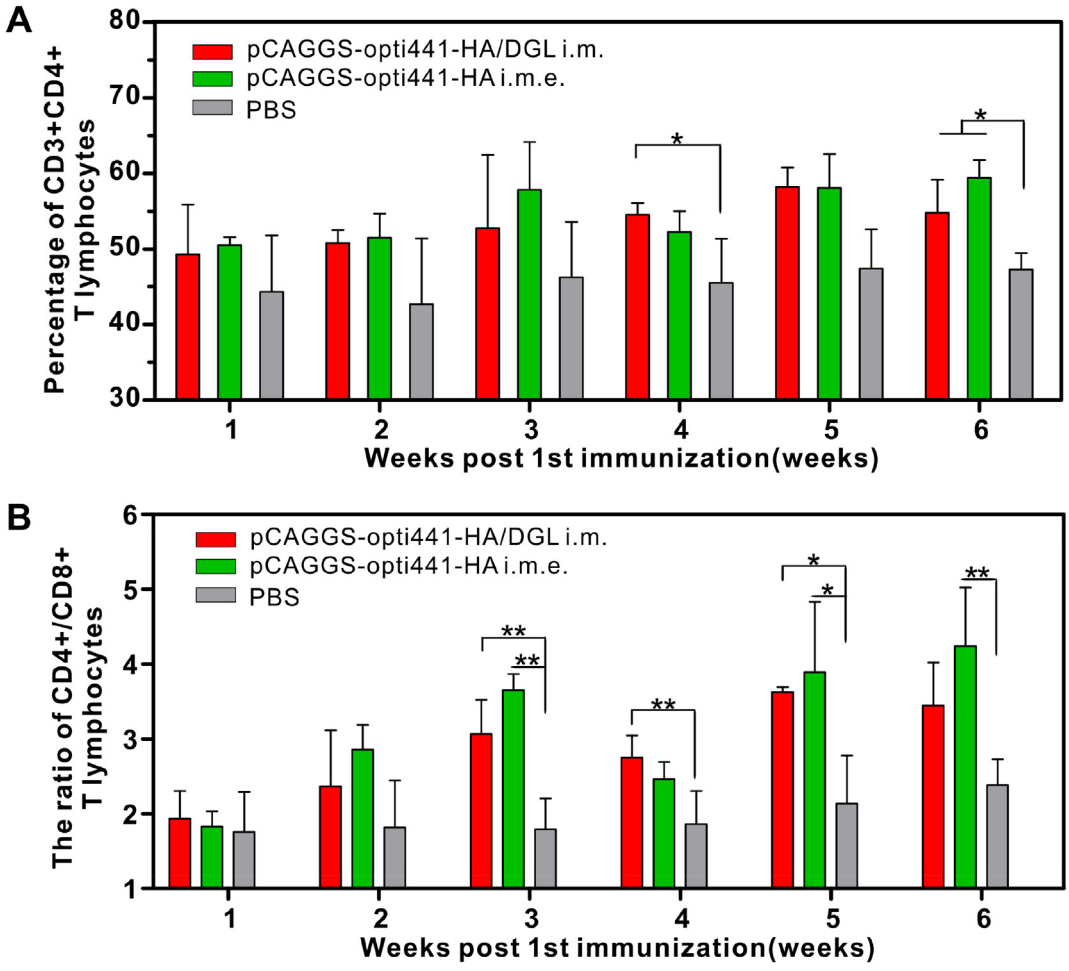

Figure 7. Changes of CD3 + CD4+ **(A)** and CD4+/CD8+ T lymphocytes **(B)** in peripheral blood post 1st immunization.

Appendix A. Supplementary data

Supplementary data to this article can be found online at https://doi.org/10.1016/j.nano.2020.102209.

References

1. Shang RF, Liang JP, Na ZY, Yang HJ, Lu Y, Hua LY, et al. *In vivo* inhibition of NAS preparation on H9N2 subtype AIV. *Virol Sin* 2010;**25**:145-50.
2. Liu D, Shi W, Gao GF. Poultry carrying H9N2 act as incubators for novel human avian influenza viruses. *Lancet* 2014;**383**:869.
3. Kadir T, Kyosuke N, Avin K. Antiviral effect of *Sanicula Europaea* L. leaves extract on influenza virus-infected cells. *Biochem Biophys Res Commun* 1996;**225**:22-6.
4. Abdulrahman A, Ghanem A. Recent advances in chromatographic purification of plasmid DNA for gene therapy and DNA vaccines: a review. *Anal Chim Acta* 2018;**1025**:41-57.
5. Munson P, Liu Y, Bratt D, Fuller JT, Hu X, Pavlakis GN, et al. Therapeutic conserved elements DNA vaccine induces strong T-cell responses against highly conserved viral sequences during simian-human immunodeficiency virus infection. *Hum Vacc Immunother* 2018;**14**:1820-31.
6. Son H, Apostolopoulos V, Chung J, Kim CW, Park J. Protective efficacy of a plasmid DNA vaccine against transgene-specific tumors by Th1 cellular immune responses after intradermal injection. *Cell Immunol* 2018;**329**:17-26.
7. Ghaffarifar F. Plasmid DNA vaccines: where are we now? *Drugs Today* 2018;**54**:315-33.
8. Liu TT, Wu Y, Niu T. Human DKK1 and human HSP70 fusion DNA vaccine induces an effective anti-tumor efficacy in murine multiple myeloma. *Oncotarget* 2018;**9**:178-91.
9. Chen YH, Yang D, Yoon YJ, Pang XC, Wang ZW, Jung JH, et al. Hairy uniform permanently ligated hollow nanoparticles with precise dimension control and tunable optical properties. *J Am Chem Soc* 2017;**139**:12956-67.
10. Delmee M, Mertz G, Bardon J, Marguier A, Ploux L, Roucoules V, et al. Laser ablation of silver in liquid organic monomer: influence of experimental parameters on the synthesized silver nanoparticles/graphite colloids. *J Phys Chem B* 2017;**121**:6646-54.
11. Hou CC, Zhu JQ. Nanoparticles and female reproductive system: how do nanoparticles affect oogenesis and embryonic development. *Oncotarget* 2017;**8**:109799-817.
12. Silva SB, Ferreira D, Pintado ME, Sarmento B. Chitosan-based nanoparticles for rosmarinic acid ocular delivery-*in vitro* tests. *Int J Biol Macromol* 2016;**84**:112-20.
13. Farjadian F, Moghoofei M, Mirkiani S, Ghasemi A, Rabiee N, Hadifar S, et al. Bacterial components as naturally inspired nano-carriers for drug/

dene delivery and immunization: set the bugs to work? *Biotechnol Adv* 2018;**36**:968-85.
14. Shirbaghaee Z, Bolhassani A. Different applications of virus-like particles in biology and medicine: vaccination and delivery systems. *Biopolymers* 2016;**105**:113-32.
15. Liu JH, Xiao J, Li F, Shi Y, Li DP, Huang QR. Chitosan-sodium alginate nanoparticle as a delivery system for epsilon-polylysine: preparation, characterization and antimicrobial activity. *Food Control* 2018;**91**:302-10.
16. Zhang C, Zhao Z, Liu GY, Li J, Wang GX, Zhu B. Immune response and protective effect against spring viremia of carp virus induced by intramuscular vaccination with a SWCNTs-DNA vaccine encoding matrix protein. *Fish Shellfish Immun* 2018;**79**:256-64.
17. Huang D, Wu DC. Biodegradable dendrimers for drug delivery. *Mat Sci Eng C-Mater* 2018;**90**:713-27.
18. Collet H, Souaid E, Cottet H, Deratani A, Boiteau L, Dessalces G, et al. An expeditious multigram-scale synthesis of lysine dendrigraft (DGL) polymers by aqueous *N*-carboxyanhydride polycondensation. *Chemistry* 2010;**16**:2309-16.
19. Li J, Liang HM, Liu J, Wang ZY. Poly (amidoamine) (PAMAM) dendrimer mediated delivery of drug and pDNA/siRNA for cancer therapy. *Int J Pharm* 2018;**546**:215-25.
20. Alemzadeh E, Dehshahri A, Izadpanah K, Ahmadi F. Plant virus nanoparticles: novel and robust nanocarriers for drug delivery and imaging. *Colloid Surface B* 2018;**167**:20-7.
21. Lancelot A, Gonzalez-Pastor R, Claveria-Gimeno R, Romero P, Abian O, Martin-Duque P, et al. Cationic poly (ester amide) dendrimers: alluring materials for biomedical applications. *J Mater Chem B* 2018;**6**:3956-68.
22. Zhao K, Li D, Cheng GG, Zhang BZ, Han JY, Chen J, et al. Targeted delivery prodigiosin to choriocarcinoma by peptide-guided dendrigraft poly-L-lysines nanoparticles. *Int J Mol Sci* 2019;**20**(21):5458.
23. Liu Y, He X, Kuang YY, An S, Wang CY, Guo YB, et al. A bacteria deriving peptide modified dendrigraft poly-L-lysines (DGL) self-assembling nanoplatform for targeted gene delivery. *Mol Pharm* 2014;**11**:3330-41.
24. Li XX, Chen J, Shen JM, Zhuang R, Zhang SQ, Zhu ZY, et al. pH-sensitive nanoparticles as smart carriers for selective intracellular drug delivery to tumor. *Int J Pharm* 2018;**545**:274-85.
25. Chen HC, Tian JW, Liu DY, He WJ, Guo ZJ. Dual aptamer modified dendrigraft poly-L-lysine nanoparticles for overcoming multi-drug resistance through mitochondrial targeting. *J Mater Chem B* 2017;**5**:972-9.
26. Tang M, Dong HQ, Li YY, Ren TB. Harnessing the PEG-cleavable strategy to balance cytotoxicity, intracellular release and the therapeutic effect of dendrigraft poly-L-lysine for cancer gene therapy. *J Mater Chem B* 2016;**4**:1284-95.
27. Kodama Y, Nakamura T, Kurosaki T, Egashira K, Mine T, Nakagawa H, et al. Biodegradable nanoparticles composed of dendrigraft poly-L-lysine for gene delivery. *Eur J Pharm Biopharm* 2014;**87**:472-9.
28. Lu ZZ, Long Y, Cun XL, Wang XH, Li JP, Mei L, et al. A size-shrinkable nanoparticle-based combined anti-tumor and anti-inflammatory strategy for enhanced cancer therapy. *Nanoscale* 2018;**10**:9957-70.
29. Mignani S, Rodrigues J, Tomas H, Caminade AM, Laurent R, Shi XY, et al. Recent therapeutic applications of the theranostic principle with dendrimers in oncology. *Sci China Mater* 2018;**61**(11):1367-86.
30. Shi C, He Y, Feng XB, Fu DH. Epsilon-polylysine and next-generation dendrigraft poly-L-lysine: chemistry, activity, and applications in biopharmaceuticals. *J Biomat Sci-Polym E* 2015;**26**:1343-56.
31. Kodama Y, Kuramoto H, Mieda Y, Muro T, Nakagawa H, Kurosaki T, et al. Application of biodegradable dendrigraft poly-L-lysine to a small interfering RNA delivery system. *J Drug Target* 2017;**25**:49-57.
32. Wang Z, Huang B, Thomas M, Sreenivasan CC, Sheng Z, Yu J, et al. Detailed mapping of the linear B cell epitopes of the hemagglutinin (HA) protein of swine influenza virus. *Virology* 2018;**522**:131-7.
33. Ba W, Chen QJ, Ze C. Complete genome sequence of an H9N2 avian influenza virus isolated from egret in lake dongting wetland. *J Virol* 2012;**86**:11939.
34. Gao YW, Zhang Y, Shinya K, Deng GH, Jiang YP, Li ZJ, et al. Identification of amino acids in HA and PB2 critical for the transmission of H5N1 avian influenza viruses in a mammalian host. *PLoS Pathog* 2009;**5**e1000709.
35. Suarez DL, Schultzcherry S. The effect of eukaryotic expression vectors and adjuvants on DNA vaccines in chickens using an avian influenza model. *Avian Dis* 2000;**44**:861-8.
36. Jiang LQ, Wang TY, Webster TJ, Duan H, Qiu JY, Zhao ZM, et al. Intracellular disposition of chitosan nanoparticles in macrophages: intracellular uptake, exocytosis, and intercellular transport. *Int J Nanomedicine* 2017;**12**:6383-98.
37. Poche RA, Hsu C, Mcelwee ML, Burns AR, Dickinson ME. Macrophages engulf endothelial cell membrane particles preceding pupillary membrane capillary regression. *Dev Biol* 2015;**403**:30-42.
38. Van Engeland NN, Bertazzo S, Sarathchandra P, Mccormack A, Bouten CC, Yacoub MH, et al. Aortic calcified particles modulate valvular endothelial and interstitial cells. *Cardiovasc Pathol* 2017;**28**:36-45.
39. Zhao L, Seth A, Wibowo N, Zhao CX, Mitter N, Yu CZ, et al. Nanoparticle vaccines. *Vaccine* 2014;**32**:327-37.
40. Parkin J, Cohen B. An overview of the immune system. *Lancet* 2001;**357**:1777-89.
41. Hutnick NA, Myles DJ, Bian CB, Muthumani K, Weiner DB. Selected approaches for increasing HIV DNA vaccine immunogenicity *in vivo*. *Curr Opin Virol* 2011;**1**:233-40.
42. Qureshi MA, Heggen CL, Hussain I. Avian macrophage: effector functions in health and disease. *Dev Comp Immunol* 2000;**24**:103-19.
43. Shiver JW, Ulmer JB, Donnelly JJ, Liu MA. Humoral and cellular immunities elicited by DNA vaccines: application to the human immunodeficiency virus and influenza. *Adv Drug Deliver Rev* 1996;**21**:19-31.
44. Hassett DE, Slifka MK, Zhang J, Whitton JL. Direct ex *vivo* kinetic and phenotypic analyses of CD8+ T-cell responses induced by DNA immunization. *J Virol* 2000;**74**:8286-91.
45. Grødeland G, Fossum E, Bogen B. Polarizing T and B cell responses by APC-targeted subunit vaccines. *Front Immuno* 2014;**6**:1-7.
46. Grødeland G, Bogen B. Efficient vaccine against pandemic influenza: combining DNA vaccination and targeted delivery to MHC class II molecules. *Expert Rev Vaccines* 2015;**14**:805-14.